

Three-Dimensional Organization of Cell Adhesion Junctions at Synapses and Dendritic Spines in Area CA1 of the Rat Hippocampus

JOSEF SPACEK¹ AND KRISTEN M. HARRIS^{2*}

¹Department of Pathology, Charles University Hospital, Hradec Kralove CZ-500-05, Czech Republic

²Division of Neuroscience in the Department of Neurology at Children's Hospital and Harvard Medical School, Boston, Massachusetts 02115

ABSTRACT

Recent work has emphasized the role of adhesion molecules in synaptic plasticity, including long-term potentiation in the hippocampus. Such adhesion molecules are concentrated in junctions that are characterized by dense thickenings on both sides of the junction and are called puncta adhaerentia (PA). Reconstruction from serial electron microscopy was used to determine the location and size of PA in the stratum radiatum of hippocampal area CA1, where many of the previous functional studies have been performed. PAs were found at the edges of synapses on 33% of dendritic spines. The areas occupied by PA were variable across different types of synapses, occupying $0.010 \pm 0.005 \mu\text{m}^2$ at macular synapses and $0.034 \pm 0.031 \mu\text{m}^2$ at perforated synapses. Another zone, called a vesicle-free transition zone (VFTZ), was identified. Like the PA, this zone also had no presynaptic vesicles and was located at the edges of synapses; however, unlike the PA, the presynaptic thickening was less than the postsynaptic thickening. Together, 45% of spine synapses had PA and/or VFTZ occupying $23 \pm 11\%$ of the total junctional area between axons and spines. PA also occurred at nonsynaptic sites involving neuronal as well as glial elements. Most (64%) of these PAs occurred between nonsynaptic portions of dendritic spines and neighboring astrocytic processes. Smooth endoplasmic reticulum was often apposed to one or both sides of the synaptic and the nonsynaptic PA. These findings provide further data as a structural basis for understanding the roles of cell adhesion junctions in hippocampal synaptic function and plasticity. *J. Comp. Neurol.* 393:58-68, 1998. © 1998 Wiley-Liss, Inc.

Indexing terms: postsynaptic density; smooth endoplasmic reticulum; astrocytes; punctum adhaerens; serial electron microscopy

In central nervous tissue, like in other epithelial tissue, the adjacent cellular elements can adhere to one another by means of specialized junctions. Two specialized adhesion junctions commonly occurring in the nervous system are the synapse and the punctum adhaerens (PA). Excitatory synapses occur on dendritic spines or directly on dendritic shafts and are characterized by an asymmetric postsynaptic density, dense staining material in the synaptic cleft, and a presynaptic clustering of vesicles in the axonal bouton. The PAs are smaller junctions that have dense thickenings on both sides of the junction with no clusters of vesicles. The PAs can occur between a wide variety of neighboring cells and processes (Peters et al., 1991). PAs have been identified among synaptic junctions in several regions of the central nervous system (Spacek,

1986, 1987; Peters et al., 1991; Lieberman and Spacek, 1997). Similar vesicle-free regions can be observed in published photomicrographs from the rat hippocampal dentate gyrus (Anthes and Petit, 1995).

The PAs have been thought to represent adhesive points that are not involved in synaptic transmission (Peters et

Grant sponsor: NIH/Fogarty International Center; Grant number: TW00178; Grant sponsor: NIH; Grant numbers: NS21184 and NS33574; Grant sponsor: MR Center; Grant number: P30-HD18655.

*Correspondence to: Kristen M. Harris, Ph.D., Division of Neuroscience, Enders 260, Children's Hospital, 300 Longwood Avenue, Boston, MA 02115. E-mail: harrisk@hub.tch.harvard.edu

Received 4 April 1997; Revised 3 November 1997; Accepted 4 November 1997

al., 1991). However, recent studies suggest that cell adhesion molecules are involved in activity-dependent synaptogenesis and synaptic plasticity, which raises the question of whether the PAs are more directly involved in signaling between synapses (for reviews, see Doherty et al., 1994; Marrs and Nelson, 1996; Fields and Ito, 1997). For example, blocking the action of cell adhesion molecules leads to deficits in learning and memory as well as a block or reduction in the magnitude of hippocampal long-term potentiation or depression (Luthi et al., 1994; Becker et al., 1996; Muller et al., 1996; Tang et al., 1996). Immunocytochemistry has revealed heavy labeling with catenins and cadherins at PA located along the borders of synaptic junctions in mouse and chick brains (Uchida et al., 1996), and confocal microscopy suggests a punctate labeling at cerebellar synapses (Fannon and Colban, 1996). In addition, synaptic junctions show immunoreactivity to the neural cell-adhesion molecule (NCAM; Pershon et al., 1989; Muller et al., 1996).

PAs have not been delineated in hippocampal area CA1 (Harris and Stevens, 1989; Harris et al., 1992; Harris and Sultan, 1995; Spacek and Harris, 1997), where many of the earlier functional studies have been performed. An important step toward understanding the function of any component in the neuropil is to have a clear description of its structural features. Hence, the goal of the present study was to determine the size and distribution of PAs in the stratum radiatum of hippocampal area CA1, thereby enhancing the structural basis for understanding how they could be involved in synaptic function.

MATERIALS AND METHODS

These analyses were performed on serial electron photomicrographs that were obtained during earlier studies in the middle of the stratum radiatum in hippocampal area CA1 (Harris and Stevens, 1989; Harris et al., 1992; Spacek and Harris, 1997). Serial sections from two young adult male rats (weighing 137 g or 310 g) of the Long-Evans strain were examined, although all of the quantitative analyses were from the larger rat. In this way, differences in the ultrastructural characteristics of the cell-adhesion junctions and synapses could not be attributed to differences in age or unsuspected differences in tissue preservation. Intracardiac perfusions were performed under deep pentobarbital (80 mg/Kg) anesthesia with fixative containing 2% paraformaldehyde, 2.5% glutaraldehyde, and 2 mM CaCl_2 in 0.1 M cacodylate buffer, pH 7.35, at 37°C and 4-psi backing pressure from compressed gas (95% O_2 , 5% CO_2). All of our procedures follow National Institutes of Health guidelines and undergo yearly review by the Animal Care and Use Committee at Children's Hospital. One hour after perfusion, the hippocampi were dissected and then sliced at 400 μm washed with slow, continuous agitation in five changes of buffer over 30–45 minutes; soaked for 1 hour in 1% OsO_4 with 1.5% $\text{K}_4\text{Fe}(\text{CN})_6$ and for 1 hour in OsO_4 ; then rinsed five times over 30 minutes in buffer and two quick changes of water. The 400- μm slices were then dehydrated through graded ethanols, including 1% uranyl acetate in the 70% ethanol for 1 hour, up to 100% ethanol (four changes for 10 minutes each), followed by propylene oxide and were embedded in Epon (equal proportions of Epon and propylene oxide overnight and then Epon at 60°C for 48 hours). Warm Epon blocks (60°C) were first hand trimmed with a razor blade and then

precision trimmed with the corner of a glass knife at room temperature on a Reichert Ultracut III ultramicrotome (Lerca, Deerfield, Illinois) to a thin trapezoid containing the CA1 pyramidal cell bodies and the entire apical dendritic arbor. One hundred and three serial sections were mounted on Formvar-coated slot grids, stained with Reynolds' lead citrate, and stored in grid cassettes for photography with a JEOL 100B electron microscope (Peabody, MA; initial magnifications of 6,600/ or 15,000/). Five different regions of these serial sections were photographed, ranging in length from 33 to 89 serial sections, and were used for three-dimensional analysis and reconstruction, as described below in Results.

This long series was supplemented with additional shorter series (<20 sections) and hundreds of individual sections from the same animal, and both uranyl acetate and lead citrate grid stains were used to enhance staining of dense thickenings for selective photography with a Telsa BS 500 electron microscope (TESCAN, Brno, Czech Republic) and to confirm observations made with lead staining alone. Lead staining alone was sufficient to see all of the features observed with both stains; however, lead alone was better for the quantitative work, because the combined stains were subject to regions of splotchy precipitate that could obscure objects of interest on serial sections.

Three-dimensional reconstructions and measurements were obtained by using PC-based software developed at Children's Hospital Image Graphics laboratory, which has been described in earlier reports (Harris and Stevens, 1989; Harris et al., 1992; Harris, 1994; Spacek, 1994; Spacek and Harris, 1997). Briefly, serial electron photomicrographs were placed under a video camera, and their images were captured in a PC-based frame grabber (Vision-8; Insync Technologies, San Leandro, CA). The images were aligned by physically moving the stage holding the electron photomicrograph of the "live" image while rapidly switching between a stored image from an adjacent section and the live image. Once the adjacent images were superimposed and stored, outlines of the plasma membrane, postsynaptic densities (PSDs), PAs, and vesicle-free transition zones (VFTZs) were traced across serial sections. A calibration grid (Pella, Redding, CA) was photographed with each series and was used to convert the pixel values to microns.

A good estimate of section thickness was needed to compute lengths, areas, and volumes across serial sections. Section thickness was set at 0.055 μm on the ultramicrotome and was then checked within the series by measuring the diameters of longitudinally sectioned mitochondria and counting the number of serial sections across which each mitochondrion appeared. Section thickness was computed as thickness ($\mu\text{m}/\text{section}$) = measured diameter/number of sections (Harris and Stevens, 1988, 1989; Harris, 1994). Eighteen mitochondria were measured to obtain the average computed section thickness of 0.055 μm , matching the setting of the ultramicrotome for this set of serial sections, which is not always the case, because section thickness can vary with many conditions during cutting (Peachey, 1958).

The areas of cross-sectioned objects (e.g., PAs and PSDs) equaled their lengths on adjacent sections multiplied by section thickness and added across sections. For *en face* PSDs, the enclosed areas were measured, and a connector was drawn to estimate where the areas overlapped in adjacent sections. The total area equaled the enclosed

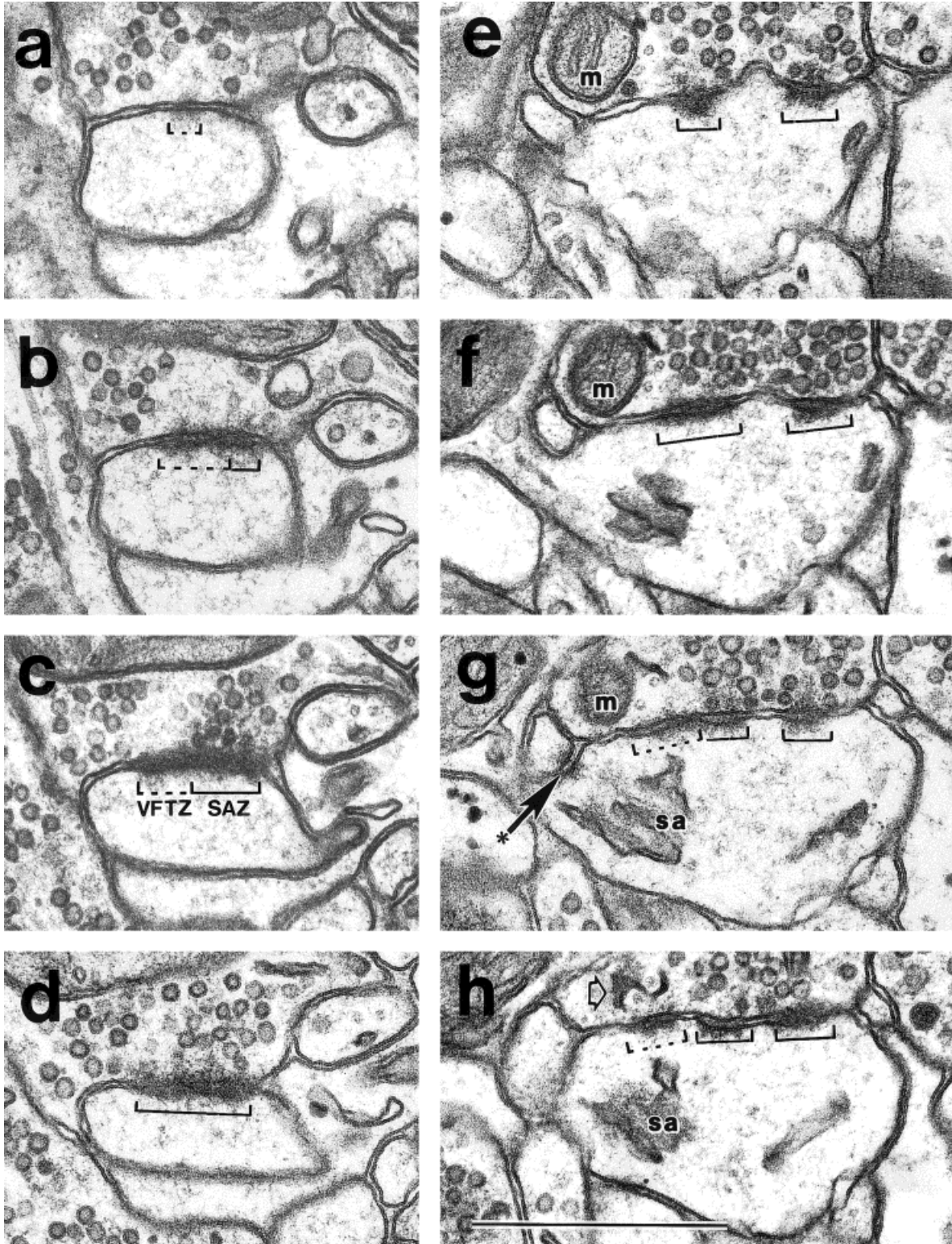


Fig. 1. Serial sections through a macular synapse (a-d) and a perforated synapse (e-h) on dendritic spines in the stratum radiatum of rat hippocampal area CA1. a-c: Serial sections through a vesicle-free transition zone (labeled VFTZ in c and bracketed with a dashed line in a-c). The VFTZ is located immediately adjacent to the synaptic active zone (labeled SAZ and bracketed by a solid line) at a macular synapse in b-d). In b-d, small synaptic vesicles and/or remnants of synaptic vesicles are docked at the SAZ, thereby distinguishing this region from the VFTZ. e-h: A VFTZ (dashed line in g and h) is distinguished from the true puncta adherentia (PA; shown in Fig.

2c,d) by the less conspicuous presynaptic density. In g, there is a nonsynaptic PA (arrow with asterisk on the left) between an astrocytic process and the spine plasma membrane. The spine apparatus (sa) is beneath the VFTZ and the nonsynaptic PA. In the presynaptic axon, a mitochondrion (m) occurs above the VFTZ and is juxtaposed to a tubule of smooth endoplasmic reticulum (SER; arrow in h), which interdigitates with two cross-sectioned microtubules. In g, the VFTZ (dashed line) is continuous with a portion of the perforated postsynaptic density (PSD) at the SAZ, the two segments of which are demarcated by solid lines in e-h. Scale bar = 0.5 μ m.

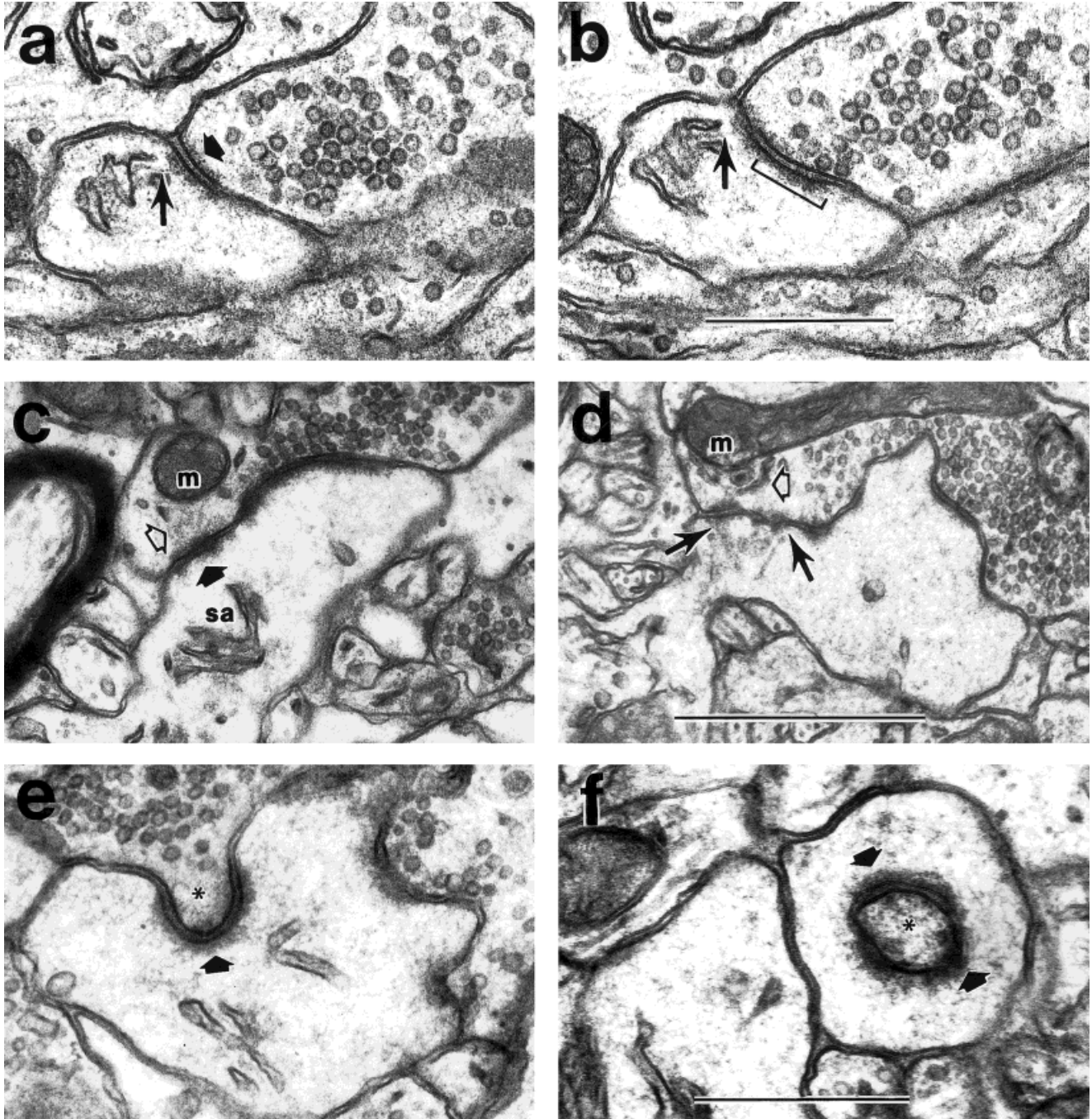


Fig. 2. Variation in the structure of puncta adhaerentia (PA) and vesicle-free transition zone (VFTZ) occurring next to synaptic active zones (SAZs). **a,b:** Serial sections through a PA that is characterized by equal, dense thickenings on the pre- and postsynaptic side. A thin filament from the dense plate (thin arrow) of the spine apparatus appears to be connected to the PA. The SAZ is delineated by a bracketed solid line in **b**, where the presynaptic vesicles are docked and clustered. The presynaptic component of PA is indicated by the thick arrow. **c:** Especially distinct PA (solid arrow) at the border of the SAZ on a mushroom spine that has a perforated postsynaptic density (PSD; perforations occur in adjacent sections not shown here) and a spine apparatus (sa). A dense-staining, microfilamentous bundle (open arrow) occurs between the presynaptic mitochondrion (m) and the presynaptic component of the PA. **d:** Several PAs occur between the solid arrows, and darkly stained filaments also emanate from a spine apparatus to the postsynaptic side of the PAs between the same two

solid arrows. The cisterns of the spine apparatus are not visible on this section. These PAs are at the edge of a perforated synapse on a mushroom-shaped dendritic spine. Smooth endoplasmic reticulum (open arrow) appears next to the PA and a mitochondrion (m) in the presynaptic axonal bouton. Synaptic vesicles are densely clustered over the SAZ of the perforated synapse on the right but are completely absent on the presynaptic side of the PA. **e,f:** Longitudinal (**e**) and cross sections (**f**) through a zone where the presynaptic axon invaginates the postsynaptic dendritic spine head (asterisk). These invaginations are surrounded by PA and VFTZ (arrows), which are distinct from the SAZ, because vesicles do not occur within the invagination. The exact delineation between the PA and the VFTZ is less distinct, because the presynaptic, dense thickenings are irregular. Scale bars = 0.5 μm in **b** (also applies to **a**), 1.0 μm in **d** (also applies to **c**), 0.5 μm in **f** (also applies to **e**).

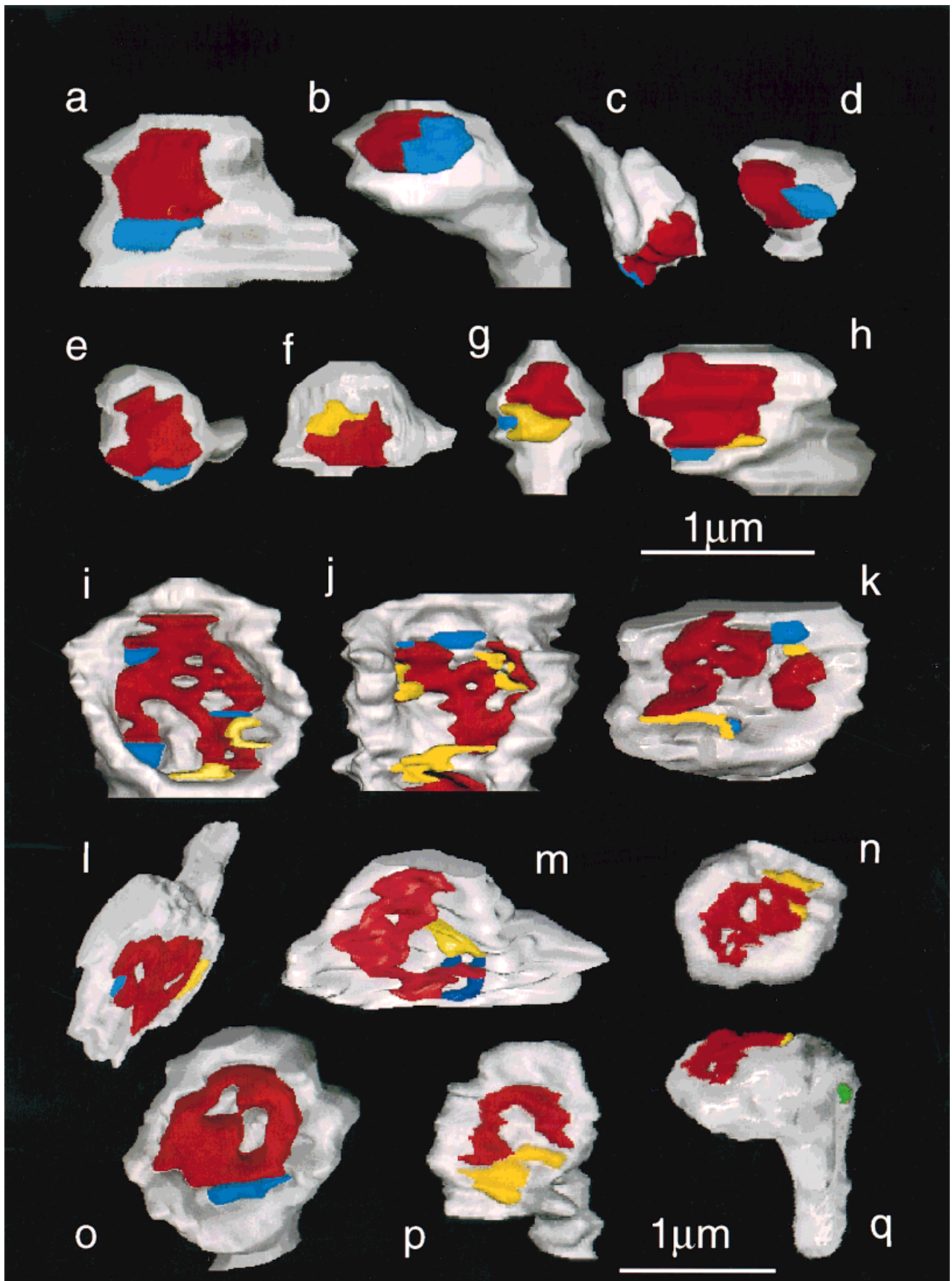


Figure 3

areas plus the length of each connector multiplied by section thickness. The nonsynaptic PAs were sufficiently small that they usually occupied only one or at most two serial sections. Hence, all of the quantitative analyses of nonsynaptic PAs were restricted to PAs that occurred in perfect cross section, as described further in Results. Three-dimensional visualization of reconstructed objects was achieved with the ICAR software (ISG Technologies, Ontario, Canada) or with a PC-based Design CAD-3D software system (American Small Business Computers, Pryor, OK; Spacek, 1994).

RESULTS

Serial electron microscopic identification of PAs and VFTZs at synaptic junctions

Synapses were evaluated through serial sections to determine their ultrastructural features. By definition, all synapses had an asymmetric synaptic active zone (SAZ; synonymous with vesicle-release zone), which was characterized by a PSD, intercellular cleft material, and an accumulation of three or more (usually hundreds) of docked and nondocked vesicles in the presynaptic bouton. The PSD was classified as macular (Fig. 1a–d) if it was continuous across serial sections of its surface or perforated if there were electron lucent regions subdividing the PSD (Figs. 1e–h, 2d).

A PA had dense thickenings on both sides of the junction, intercellular cleft material, and an absence of presynaptic vesicles (Fig. 2a,c,d). Another zone, a VFTZ, was also identified at many synapses. Like the PA, this zone had a PSD, intercellular cleft material, and no cluster of presynaptic vesicles; however, there was a less conspicuous, dense thickening on the axonal side of the junction (compare the VFTZ in Fig. 1a–c,g,h with the PA in Fig. 2c,d). At some synapses, it was quite difficult to distinguish the PA from the VFTZ (e.g., Fig. 2e,f), although the absence of presynaptic vesicles distinguished both PA and VFTZ from the SAZ. The criterion for determining an absence of presynaptic vesicles was that vesicles were not found hovering within approximately two vesicle diameters of the presynaptic site. It should be noted, however, that the nondocked vesicles were usually farther removed from the PA than just two diameters (see, e.g., Fig. 2c,d). Obviously, there were also no docked vesicles at the PA or the VFTZ. Docked vesicles tend to be smaller than nondocked vesicles (Harris and Sultan, 1995). Tangentially sectioned docked vesicles or their remnants also were not seen in the VFTZ, which, for example, distinguishes the VFTZ in Figure 1c from the left edge of the SAZ in Figure 1d.

The three-dimensional reconstructions of dendritic spines in Figure 3 (gray) illustrate that the PA (blue) and VFTZ (yellow) are always located at the edges of the SAZ (red).

This consistent occurrence of the PA and VFTZ at the edges of the SAZ suggests that they are not random artifacts created by vesicular release during fixation, because, if this were so, then one would expect to see them distributed equally throughout the SAZ. The presence of vesicles at the SAZ and absence at the PA and VFTZ suggest that the SAZ is functionally distinct from these other two zones. Whether the VFTZs are functionally as well as structurally transitional between the PA and the SAZ remains to be determined.

All of the synapses transected by the middle section of one of the photomicrographic series (K34; 33 serial sections) were traced through serial sections to determine whether the synapse was macular or perforated and whether it had a PA, a VFTZ, or both. In this way, we did not preselect a particular synapse for the occurrence or absence of PAs or VFTZs, and we were able to determine the relative frequencies of PAs and VFTZs at the two main types of synapses (macular or perforated).

A total of 94 synapses were examined in this analysis, and 42 had PAs or VFTZs (i.e., 45% of all synapses; Table 1). Of the 68 macular synapses, 32% had PAs or VFTZs, whereas 77% of the 26 perforated PSDs had PAs or VFTZs. All 42 of these synapses with PAs or VFTZs were reconstructed to measure the relative areas of the SAZs, PAs, and VFTZs (Table 1). The surface areas of the PAs plus the VFTZs occupied $23 \pm 11\%$ of the synaptic junctional area. A linear-regression analysis shows a negative trend toward a lesser percentage of the junctional area being occupied by PAs or VFTZs at the larger perforated synapses than at the smaller macular synapses (Fig. 4), even though the absolute areas of the PAs and/or VFTZs were larger at the perforated synapses (Table 1).

Nonsynaptic PAs

All five sets of serial sections, containing a total volume of $1,124 \mu\text{m}^3$, were examined thoroughly for the presence of PAs at nonsynaptic sites by systematically viewing the plasmalemmal outlines of all neuronal and glial elements. Each series was searched a minimum of two times. Only PAs that were cut perfectly transversely were counted, because the identity of obliquely cut PAs was not clear.

In total, 66 transverse PAs were identified. This number certainly does not represent all of the PAs that existed in this volume of neuropil, because many more were also likely to be obliquely sectioned. Due to this problem of identifying an obliquely sectioned PA, we can think of no way to obtain an accurate absolute frequency for PAs in the neuropil. There is no reason to believe that PAs on some types of elements were more likely to be cross sectioned than PAs on other elements; hence, the relative percentages of PAs between different neuronal and/or glial elements should be representative of their occurrence throughout the neuropil.

Most (64%) of these nonsynaptic PAs occurred between dendritic spines and neighboring astrocytic processes (Fig. 1g; Fig. 3q, green spot; Figs. 5, 6). In addition, 20% of the PAs occurred between astrocytic processes and dendritic shafts, and the remaining 16% of the PAs were distributed among adjacent axon terminals, dendritic spines, dendritic shafts, and astrocytic processes at nonsynaptic sites (Fig. 6). None of these nonsynaptic PAs spanned more than two sections, and they usually did not span more than one section; hence, they were smaller than the typical synaptic PAs. The diameters were measured for all 66 of these PAs and ranged from $0.032 \mu\text{m}$ to $0.135 \mu\text{m}$ (mean \pm S.D.; $0.067 \pm 0.019 \mu\text{m}$; i.e., approximately

Fig. 3. Representative three-dimensional reconstructions of different types of synaptic junctions on dendritic spines. **a–h**: Macular synapses on large and small dendritic spines. **i–q**: Perforated synapses on large dendritic spines. The puncta adhaerentia (PAs; shown in blue) were either at the edge of the vesicle-free transition zone (VFTZ; yellow), at the edge of the synaptic active zone (SAZ; red), or both. Complete perforations occurred only in the SAZ (gray areas surrounded by red) or could appear to be created by the contiguity of one or more zones. In **q**, the green spot toward the right illustrates a PA between the spine plasma membrane and a neighboring astrocytic process (see also Fig. 5). Top scale bar is for **a–h** and bottom scale bar is for **i–q**.

TABLE 1. Frequency and Dimensions of Synaptic Junctions With Puncta Adhaerentia and/or Vesicle-Free Transition Zones¹

Synapse type	Total no.	No. with PA or VFTZ	No. with PA only	No. with VFTZ only	No. with both PA and VFTZ	SAZ area (μm^2) mean \pm S.D.	PA area (μm^2) mean \pm S.D.	VFTZ area (μm^2) mean \pm S.D.
Total	94	42	13	11	18	—	—	—
Macular	68	22	9	10	3	0.06 \pm 0.04	0.01 \pm 0.005	0.01 \pm 0.005
Perforated	26	20	4	1	15	0.39 \pm 0.19	0.034 \pm 0.031	0.046 \pm 0.033

¹PA, puncta adhaerentia; VFTZ, vesicle-free transition zone; SAZ, synaptic active zone.

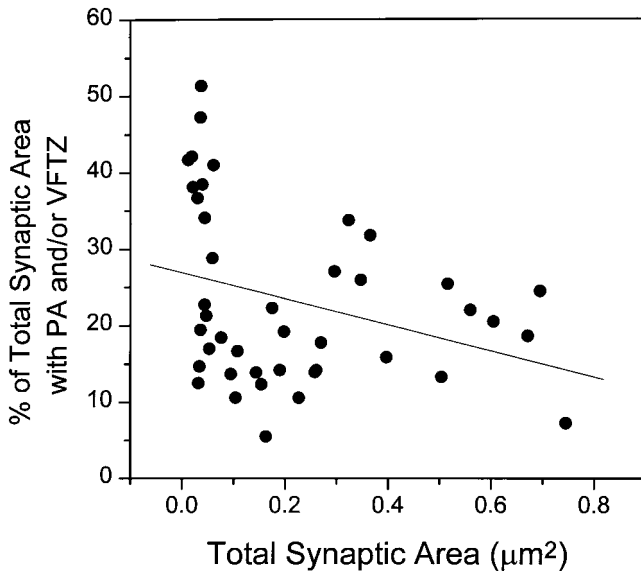


Fig. 4. Percentage of the synaptic junction that is occupied by puncta adhaerentia (PA) and/or vesicle-free transition zone (VFTZ). Although the actual area occupied by PA and VFTZ was greater at larger synapses (see Table 2), the percentage occupancy was less at the larger synapses (linear regression: $r = -0.32$; $n = 42$; $P < 0.05$). In this graph, the smallest 22 synapses ($\leq 0.15 \mu\text{m}^2$) are macular, and the largest 20 synapses ($> 0.15 \mu\text{m}^2$) are perforated.

$0.004 \pm 0.001 \mu\text{m}^2$ when multiplied by the section thickness of $0.055 \mu\text{m}$).

Association between PAs and smooth endoplasmic reticulum

During the analysis of nonsynaptic PAs, another 107 synaptic junctions (66 macular and 41 perforated synapses on dendritic spines) were identified that had PAs and/or VFTZs. In addition, the PAs and/or VFTZs were also observed at four asymmetric and four symmetric synapses on the dendritic shafts as well as at one axosomatic synaptic junction. These are not all of the synapses in this volume of neuropil that might have had PAs and/or VFTZs: They simply represent an additional population that was discovered during the analysis of nonsynaptic PAs. These new synapses, together with the 42 synapses from the unbiased quantitative analysis of macular and perforated synapses discussed above, and the nonsynaptic PAs were viewed through serial sections to determine the juxtaposition of PAs and/or VFTZs with other organelles.

At both synaptic and nonsynaptic PAs, smooth endoplasmic reticulum (SER), mitochondria, and the spine apparatus (SA) or its dense plate (DP) material could be found adjacent to the PA on one or both sides of the membrane. A tubule of SER or cistern from the SA was adjacent to the PA at 48% of the perforated synapses (see, e.g., Figs. 1g,h, 2a-d); however, none of the macular synapses showed any

evidence of SER next to the PA (Table 2, top). On the presynaptic side, the fine structure of the PA was not as clearly apparent due to the denser cytoplasmic background; nevertheless, filaments were also observed emanating from the dense material of the PA to SER on the presynaptic side (see, e.g., Figs. 1h, 2d). A mitochondrion or a bundle of filaments emanating from the mitochondrion could also be observed at the PA on the presynaptic side (Fig. 2c). When PAs occurred at nonsynaptic sites, SER or part of the SA was juxtaposed with the PA in 69% of the dendritic spines, in 29% of the astrocytic processes (see, e.g., Fig. 5b), in 29% of the dendritic shafts, and in 55% of the axon terminals (Table 2, bottom).

DISCUSSION

These results show that almost half of the synapses occurring on hippocampal dendritic spines have specialized junctions (PAs and/or VFTZs) at the edges of the SAZ. All sizes and shapes of synaptic junctions can have PAs and/or VFTZs. These observations raise the questions of whether the PAs and VFTZs are 1) functionally separate units; 2) precursors to the PSD, which will become the active zone; or 3) a product of synaptic remodeling at these adult synapses (Itarat and Jones, 1993). PAs might serve multiple functions. If PAs stabilize a synapse structurally, then they might need to be broken to allow synaptic remodeling in much the same way that cell-adhesion molecules need to be endocytosed prior to axonal sprouting and synaptic plasticity at *Aplysia* neurons (Bailey et al., 1997). If cell-adhesion molecules localized to PAs enhance calcium influx at hippocampal dendritic spine synapses, then both synaptic and astroglial elements could respond during synaptic transmission via PAs at many, but not all, spine synapses. The absence of synaptic vesicles at the PAs and VFTZs strongly suggests that they are functionally distinct from the SAZs, where synaptic vesicles are presumably released. Future studies will be needed to determine whether the PAs and VFTZs are functionally distinct from one another and whether they respond to specific patterns of synaptic activation.

The appearance and size of the hippocampal PAs and VFTZs are similar if not identical to those found at synapses in other brain regions (Spacek, 1986; Anthes and Petit, 1995). Early during development, surface specializations occur between growth cones and neural processes that are also structurally similar to the PAs and are thought to be involved in early synaptogenesis as well as in the stabilization of appropriate synaptic connections (Dyson and Jones, 1976, 1984; Rees, 1978; Blue and Parnavelas, 1983; Vaughn, 1989; Rose et al., 1995; Bahjaoui-Bouhaddi et al., 1997; Inoue and Sanes, 1997; personal observations in developing hippocampus). Recent electron microscopic immunogold labeling suggests that the PAs are functionally separate from the SAZ (Uchida et al., 1996). The n-cadherin/catenin system of cell-adhesion

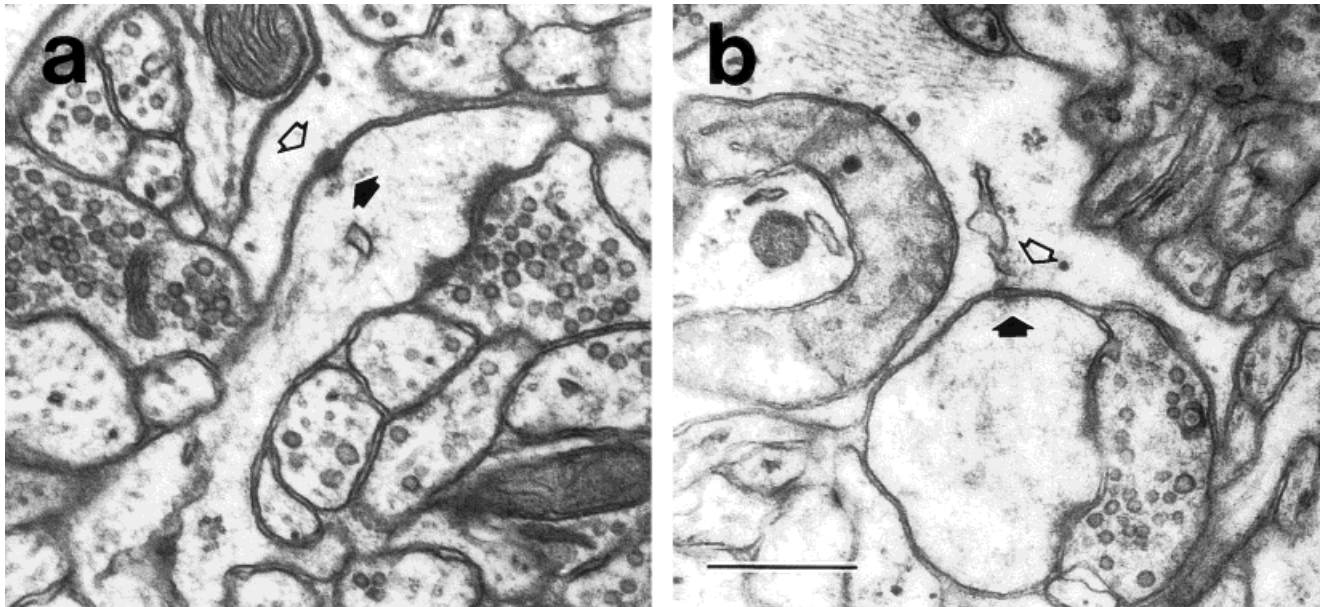


Fig. 5. **a,b:** Puncta adhaerentia (PA) between nonsynaptic portions of the plasma membranes of dendritic spines (solid arrows) and neighboring astrocytic processes (open arrows). In b, a tubule of smooth endoplasmic reticulum (SER) is adjacent to the PA on the astrocytic side (open arrow). Scale bar = 0.5 μ m.

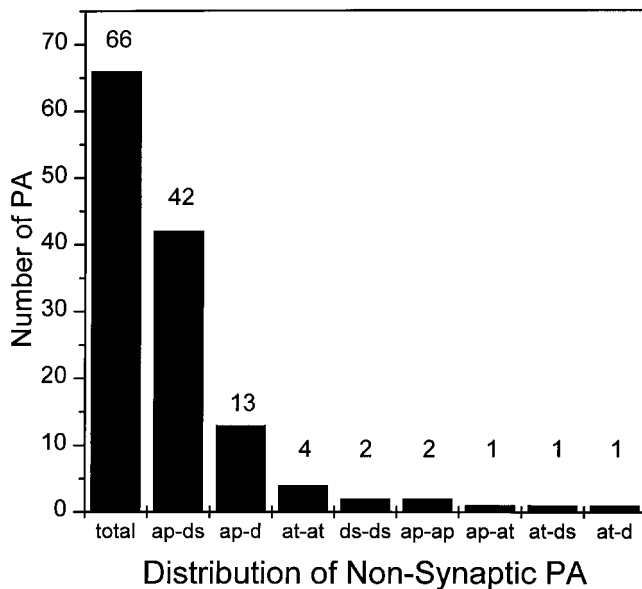


Fig. 6. Distribution of nonsynaptic puncta adhaerentia (PA). ap, Astrocytic process; ds, dendritic spine; d, dendritic shaft; at, axon terminal.

molecules was localized specifically in PA-like structures bordering transmitter-release zones (i.e., the SAZ) of mature cerebellar and cortical synapses in chick and mouse brains. In that material, the PAs bordering the synapses were similar to the PAs we observed bordering the hippocampal synapses. Hence, it seems that, even though PAs might be especially important during early synaptogenesis, they may also remain as functionally distinct units at mature synaptic complexes.

TABLE 2. Associations Between Puncta Adhaerentia and Smooth Endoplasmic Reticulum or the Spine Apparatus¹

Location of PA	Total	No. assoc. with SER	No. assoc. with SA	No. assoc. with DP	% Total
Synaptic					
Macular	88	0	0	0	0
Perforated	61	7	21	1	48
Nonsynaptic					
Spine side	48	5	13	4	46
Astrocytic side	61	17	—	—	28
Dendritic shaft side	14	4	—	—	29
Axonal terminal side	11	6	—	—	54

¹For the nonsynaptic puncta adhaerentia (PA) the total number is greater than 66, because smooth endoplasmic reticulum (SER) could occur on one or both sides of the junction. SA, spine apparatus; DP, dense plate.

PAs occurring between like processes, such as between neighboring dendrites, have the same thickness on both sides; however, PAs occurring between dissimilar processes, such as between axons and dendrites, have different degrees of thickness on the two sides of the adhesion (Lieberman and Spacek, 1997). This asymmetry in the PAs and VFTZs was also seen at the hippocampal synapses, where the adhesion was usually thinner on the axonal than on the dendritic spine side. These observations suggest that the structural heterogeneity of the PAs and VFTZs might result from a molecular heterogeneity among adhesion molecules localized to different parts of the same cell or to different cell types.

The postsynaptic thickening at the VFTZ is similar in appearance to the PSD at the SAZ. If this similarity in structure reflects a similar molecular composition, then the VFTZs might be a readily available source of PSD. In addition, the location of VFTZs at the edges of SAZs could allow for the rapid recruitment or loss of synaptic receptive area in association with enhanced or reduced synaptic strength during periods of synaptic plasticity, such as long-term potentiation or depression.

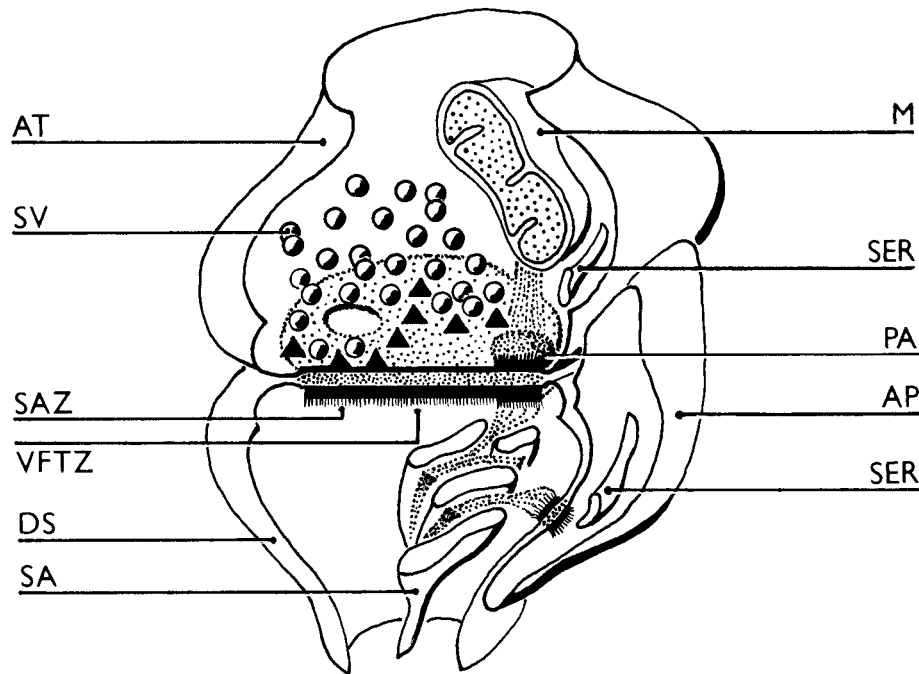


Fig. 7. Diagrammatic representation of the different components of a perforated synaptic complex. The perforated synaptic active zone (SAZ), vesicle-free transition zone (VFTZ), and puncta adhaerentia (PA) are located on a large dendritic spine (DS) that contains a spine apparatus (SA) from which the dense plates are connected to both the PA at the synapse and the PA at the astrocytic process (AP). The

perforation in the SAZ is represented by the open area in the stippling. The presynaptic axon terminal (AT) contains many synaptic vesicles (SV) as well as a mitochondrion (M) and smooth endoplasmic reticulum (SER), both of which are connected by filaments to the PA. The astrocytic process also contains SER next to the PA.

By using confocal microscopy, Fannon and Colban (1996) proposed a model whereby cadherin molecules localized in punctate structures at cerebellar and hippocampal synapses would be the structural correlate of the perforated PSD. In their model, the cadherins would adhere the PSD to the presynaptic axon, and presynaptic vesicles would aggregate at a perforation in the middle of the PSD (see Fannon and Colban, 1996). Reconstructions of perforated synapses argue against such a model. Instead, perforations in the PSD are surrounded by the SAZ, and vesicles cluster preferentially at the presynaptic zone across from the PSD, not only at the zone across from the perforation(s), as depicted by Fannon and Colban (1996); instead, see Figures 1, 2, and 5 of this paper as well as Harris and Sultan (1995) and Spacek and Harris (1997). Furthermore, because well-formed PAs are also found at the edges of both perforated and macular synapses, perforations are not correlated with the occurrence of PAs where cell-adhesion molecules are likely to be localized. Together, these findings suggest instead that the punctate appearance of the cadherin staining observed with confocal microscopy is due to the occurrence of PA at the edges of the synapses and not to perforations in the PSD at SAZs. Figure 7 illustrates a more realistic model of a perforated synaptic complex, including PAs and VFTZs, based on the three-dimensional analyses obtained in this study and the electron microscopic localization of cell-adhesion molecules obtained elsewhere (Uchida et al., 1996).

The close proximity of the postsynaptic SA to the PAs and VFTZs has also been observed in earlier studies (Tarrant and Routtenberg, 1979; Westrum et al., 1980; Dyson and Jones, 1984; Spacek, 1985, 1986; Spacek and

Harris, 1997). The filaments emanating from the SA are likely to contain actin and MAP2 (Morales and Fifkova, 1989); Whether they contain other molecules destined for the PA or synapse remains to be determined. Presynaptically, filaments radiated between the PA and the mitochondria or SER, an observation that has been made at other synapses (Spacek, 1986, 1987; Hirokawa et al., 1989), as well as more generally at the PA between epithelial cells in various tissues (Altorfer et al., 1974; Bernstein and Wollman, 1975, 1976; Freddo, 1988). PAs were also observed between dendritic spines and neighboring astrocytic processes. Here, too, the SER and/or components of the SA were often continuous with either side of the PA. Because cell-cell adhesion molecules can affect the regulation of calcium (Fields and Ito, 1997), the close association of SER with the PA might provide a mechanism whereby synaptic activation at dendritic spines could initiate a calcium signal both in the postsynaptic dendritic spine as well as in neighboring astroglia (Finkbeiner, 1995; Porter and McCarthy, 1996; Verkhratsky and Kettenmann, 1996; Linden, 1997).

Do the ~50% of hippocampal synapses with PA and/or VFTZ represent functionally distinct populations of synapses from those without PA and/or VFTZ? Because all types of synapses were found to have PA and/or VFTZ, it seems unlikely that they are peculiar to a particular type of synapse; instead, it seems that their presence or absence might reflect the history of activation at an individual synapse. Recent studies provide evidence that at least two different cell-adhesion molecules, NCAM and cadherin, are involved in hippocampal synaptic plasticity (Luthi et

al., 1994; Becker et al., 1996; Muller et al., 1996; Tang et al., 1996). When polysialic acid is cleaved from NCAM, making it more adhesive, neither long-term potentiation (LTP) nor long-term depression (LTD) occurs, suggesting that less adhesive synapses are more plastic (Luthi et al., 1994; Muller et al., 1996). Antibodies to cadherin also interfere with cell adhesion, which should make the synapses less adhesive and more plastic; however, this intervention also reduces LTP (Tang et al., 1996). Thus, the second-messenger signaling via cell-adhesion molecules, which requires the adhesion to be intact, could also be important for LTP. Further study will be needed to sort out exactly where the different adhesion molecules are located at hippocampal synapses. The preferential location of PAs and VFTZs at synaptic borders and between spines and astrocytes suggests that they could prove to be intriguing candidates in the exploration of cellular and structural mechanisms of synaptic function and plasticity in the hippocampus.

ACKNOWLEDGMENTS

We thank Dr. John Fiala for assistance on the reconstruction systems in the Image Graphics laboratory at Children's Hospital. We also thank John Fiala, Karin Sorra, and Mireya Nadel-Vicens for comments on the paper.

LITERATURE CITED

- Altorfer, J., T. Fukuda, and C. Hedinger (1974) Desmosomes in human seminiferous epithelium. *Virchow's Arch. B. Cell Pathol.* 16:181-194.
- Anthes, D.L. and T.L. Petit (1995) A new morphological feature associated with perforated synapses: Vesicular lateralization. *Synapse* 19:294-296.
- Bahjaoui-Bouhaddi, M., F. Padilla, M. Nicolet, C. Cifuentes-Diaz, D. Fellmann, and R.M. Mege (1997) Localized deposition of M-cadherin in the glomeruli of the granular layer during the postnatal development of mouse cerebellum. *J. Comp. Neurol.* 378:180-195.
- Bailey, C.H., B.K. Kaang, M. Chen, K.C. Martin, C.S. Lim, A. Casadio, and E.R. Kandel (1997) Mutation in the phosphorylation sites of MAP kinase blocks learning-related internalization of apCAM in Aplysia sensory neurons [see comments]. *Neuron* 18:913-924.
- Becker, C.G., A. Artola, R. Gerardy-Schahn, T. Becker, H. Welzl, and M. Schachner (1996) The polysialic acid modification of the neural cell adhesion molecule is involved in spatial learning and hippocampal long-term potentiation. *J. Neurosci. Res.* 45:143-152.
- Bernstein, L.H. and S.H. Wollman (1975) Association of mitochondria with desmosomes in the rat thyroid gland. *J. Ultrastructure Res.* 53:87-92.
- Bernstein, L.H. and S.H. Wollman (1976) A circumferential bundle of microfilaments associated with desmosomes near apex of typical thyroid epithelial cells. *J. Ultrastructure Res.* 56:326-330.
- Blue, M.E. and J.G. Parnavelas (1983) The formation and maturation of synapses in the visual cortex of the rat. I. Qualitative analysis. *J. Neurocytol.* 12:599-616.
- Doherty, P., M.S. Fazeli, and F.S. Walsh (1994) The neural cell adhesion molecule and synaptic plasticity. *J. Neurobiol.* 26:437-446.
- Dyson, S.E. and D.G. Jones (1976) The morphological categories of developing synapses. *Cell Tissue Res.* 167:363-371.
- Dyson, S.E. and D.G. Jones (1984) Synaptic remodeling during development and maturation: Junction differentiation and splitting as a mechanism for modifying connectivity. *Dev. Brain Res.* 13:125-137.
- Fannon, A.M. and D.R. Colban (1996) A model for central synaptic junctional complex formation based on the differential adhesive specificities of the cadherins. *Neuron* 17:423-434.
- Fields, R.D. and K. Ito (1997) Neural cell adhesion molecule in activity-dependent development and synaptic plasticity. *Trends Neurosci.* 19:473-480.
- Finkbeiner, S.M. (1995) Modulation and control of intracellular calcium. In H. Kettenmann and B.R. Ransom (eds): *Neuroglia*. New York, NY: Oxford University Press, pp. 273-288.
- Freddo, T.F. (1988) Mitochondria attached to desmosomes in the ciliary epithelia of human, monkey, and rabbit eyes. *Cell Tissue Res.* 251:671-675.
- Harris, K.M. (1994) Serial electron microscopy as an alternative or complement to confocal microscopy for the study of synapses and dendritic spines in the central nervous system. In J.K. Stevens, L.R. Mills, and J.E. Trogadis (eds): *Three-Dimensional Confocal Microscopy: Volume Investigation of Biological Specimens*. New York, NY: Academic Press, Inc. pp. 421-445.
- Harris, K.M. and J.K. Stevens (1989) Dendritic spines of CA1 pyramidal cells in the rat hippocampus: Serial electron microscopy with reference to their biophysical characteristics. *J. Neurosci.* 9:2982-2997.
- Harris, K.M. and P. Sultan (1995) Variation in number, location, and size of synaptic vesicles provides an anatomical basis for the nonuniform probability of release at hippocampal CA1 synapses. *J. Neuropharmacol.* 34:1387-1395.
- Harris, K.M., F.E. Jensen, and B. Tsao (1992) Three-dimensional structure of dendritic spines and synapses in rat hippocampus (CA1) at postnatal day 15 and adult ages: Implications for the maturation of synaptic physiology and long-term potentiation. *J. Neurosci.* 12:2685-2705.
- Hirokawa, N., K. Sobue, K. Kanda, A. Harada, and H. Yorifuji (1989) The cytoskeletal architecture of the presynaptic terminal and molecular structure of synapsin I. *J. Cell Biol.* 108:111-126.
- Inoue, A. and J.R. Sanes (1997) Lamina-specific connectivity in the brain: Regulation by N-cadherin, neurotrophins, and glycoconjugates. *Science* 276:1428-1431.
- Itarat, W. and D.G. Jones (1993) Morphological characteristics of perforated synapses in the latter stages of synaptogenesis in rat neocortex: Stereological and three-dimensional approaches. *J. Neurocytol.* 22:753-764.
- Lieberman, A.R. and J. Spacek (1997) Filamentous contacts: The ultrastructure and three-dimensional organization of specialized nonsynaptic interneuronal appositions in thalamic relay nuclei. *Cell Tissue Res.* 288:43-57.
- Linden, D.J. (1997) Long-term potentiation of glial synaptic currents in cerebellar culture. *Neuron* 18:983-994.
- Luthi, A., J.P. Laurent, A. Figuero, D. Muller, and M. Schachner (1994) Hippocampal long-term potentiation and neural cell adhesion molecules L1 and NCAM. *Nature* 372:777-779.
- Marrs, J.A. and W.J. Nelson (1996) Cadherin cell adhesion molecules in differentiation and embryogenesis. *Int. Rev. Cytol.* 165:159-205.
- Morales, M. and E. Fifkova (1989) Distribution of MAP 2 in dendritic spines and its colocalization with actin. An immunogold electron-microscope study. *Cell Tissue Res.* 256:447-456.
- Muller, D., C. Wang, G. Skibo, N. Toni, H. Cremer, V. Calaora, G. Rougon, and J.Z. Kiss (1996) PSA-NCAM is required for activity-induced synaptic plasticity. *Neuron* 17:413-422.
- Peachey, L.D. (1958) A study of section thickness and physical distortion produced during microtomy. *J. Biophys. Biochem. Cytol.* 4:233-242.
- Pershon, E., G.E. Pollerberg, and M. Schachner (1989) Immunoelectron-microscopic localization of the 180 kD component of the neural cell adhesion molecule N-CAM in postsynaptic membranes. *J. Comp. Neurol.* 288:92-100.
- Peters, A., S.L. Palay, and H.D. Webster (1991) *The Fine Structure of the Nervous System: The Neurons and Supporting Cells*. Philadelphia, PA: W.B. Saunders Co.
- Porter, J.T. and K.D. McCarthy (1996) Hippocampal astrocytes in situ respond to glutamate released from synaptic terminals. *J. Neurosci.* 16:5073-5081.
- Rees, R. (1978) The morphology of interneuronal synaptogenesis: A review. *Am. Soc. Exp. Biol.* 37:2000-2009.
- Rose, O., C. Grund, S. Reinhardt, A. Starzinski-Powitz, and W.W. Franke (1995) Contactus adherens, a special type of plaque-bearing adhering junction containing M-cadherin, in the granule cell layer of the cerebellar glomerulus. *Proc. Natl. Acad. Sci. USA* 92:6022-6026.
- Spacek, J. (1985) Three-dimensional analysis of dendritic spines. II. Spine apparatus and other cytoplasmic components. *Anat. Embryol.* 171:235-243.
- Spacek, J. (1986) Relationships between synaptic junctions, puncta adherentia and the spine apparatus at neocortical axo-spinous synapses. *Anat. Embryol.* 173:129-135.

- Spacek, J. (1987) Ultrastructural pathology of dendritic spines in epitemorous human cerebral cortex. *Acta Neuropathol. (Berlin)* 73:77–85.
- Spacek, J. (1994) Design CAD-3D: A useful tool for 3-dimensional reconstructions in biology [letter]. *J. Neurosci. Methods* 53:123–124.
- Spacek, J. and K.M. Harris (1997) Three-dimensional organization of smooth endoplasmic reticulum in hippocampal CA1 dendrites and dendritic spines of the immature and mature rat. *J. Neurosci.* 17:190–203.
- Tang, L., C.P. Hung, and E.M. Schuman (1996) Role of cadherin molecules in synaptic plasticity in the adult rat hippocampus. *Soc. Neurosci. Abstr.* 22:332.
- Tarrant, S.B. and A. Routtenberg (1979) Postsynaptic membrane and spine apparatus: Proximity in dendritic spines. *Neurosci. Lett.* 11:289–294.
- Uchida, N., Y. Honjo, K.R. Johnson, M.J. Wheelock, and M. Takeichi (1996) The catenin/cadherin adhesion system is localized in synaptic junctions bordering transmitter release zones. *J. Cell Biol.* 135:767–779.
- Vaughn, J.E. (1989) Review: Fine structure of synaptogenesis in vertebrate central nervous system. *Synapse* 3:255–285.
- Verkhatsky, A., and H. Kettenmann (1996) Calcium signaling in glial cells. *Trends Neurosci.* 19:346–352.
- Westrum, L.E., D.H. Jones, E.G. Gray, and J. Barron (1980) Microtubules, dendritic spines and spine apparatuses. *Cell Tissue Res.* 208:171–181.